ESC European Society of Cardiology

Cardiovascular Research (2022) **118**, 913–928
doi:10.1093/cvr/cvab107

SPARC-related modular calcium binding 1 regulates aortic valve calcification by disrupting BMPR-II/p-p38 signalling

Yaqing Wang[1†], Jia Gu[1†], Anning Du [1†], Siqi Zhang[1†], Mengqing Deng[1], Rong Zhao [2], Yan Lu[1], Yue Ji[1], Yongfeng Shao[3], Wei Sun [1*], and Xiangqing Kong[1,4*]

[1]Department of Cardiology, The First Affiliated Hospital of Nanjing Medical University, 300 Guangzhou Road, Nanjing 210029, PR China; [2]Department of Cardiology, The First People's Hospital of Changzhou, 185 Juqian Street, Changzhou 213004, PR China; [3]Department of Cardiovascular Surgery, The First Affiliated Hospital of Nanjing Medical University, 300 Guangzhou Road, Nanjing 210029, PR China; [4]State Key Laboratory of Reproductive Medicine, Nanjing Medical University, 101 Longmian Avenue, Nanjing 210029, PR China

Received 21 April 2020; editorial decision 13 March 2021; accepted 21 March 2021; online publish-ahead-of-print 23 March 2021

Time for primary review: 27 days

Aims Aortic valve calcification is more prevalent in chronic kidney disease accompanied by hypercalcemia. Secreted protein acidic and rich in cysteine (SPARC)-related modular calcium binding 1 (SMOC1) is a regulator of BMP2 signalling, but the role of SMOC1 in aortic valve calcification under different conditions has not been studied. This study aimed to investigate the roles of SMOC1 in aortic valve calcification under normal and high calcium conditions, focusing on the effects on aortic valve interstitial cells (AVICs).

Methods and results SMOC1 was expressed by aortic valve endothelial cells and secreted into the extracellular matrix in non-calcific valves and downregulated in calcific aortic valves. *In vitro* studies demonstrated that HUVEC secreted SMOC1 could enter the cytoplasm of AVICs. Overexpression of SMOC1 attenuated warfarin-induced AVIC calcification but promoted high calcium/phosphate or vitamin D-induced AVIC and aortic valve calcification by regulating BMP2 signalling both *in vitro* and *in vivo*. Co-immunoprecipitation revealed that SMOC1 binds to BMP receptor II (BMPR-II) and inhibits BMP2-induced phosphorylation of p38 (p-p38) via amino acids 372–383 of its EF-hand calcium-binding domain. Inhibition of p-p38 by the p38 inhibitor SB203580 blocked the effects of SMOC1 on BMP2 signalling and AVIC calcification induced by high calcium/phosphate medium. In high-calcium-treated AVICs, SMOC1 lost its ability to bind to BMPR-II, but not to caveolin-1, promoting p-p38 and cell apoptosis due to increased expression of BMPR-II and enhanced endocytosis.

Conclusions These observations support that SMOC1 works as a dual-directional modulator of AVIC calcification by regulating p38-dependent BMP2 signalling transduction according to different extracellular calcium concentrations.

*Corresponding authors. Tel: +(86) 2568303837; fax: +(86) 2568303837, E-mail: weisun7919@njmu.edu.cn (W.S.); Tel: +(86) 2568303837; fax: +(86) 2568303837, E-mail: Kongxq@njmu.edu.cn (X.K.)

†These authors contributed equally to this work.

Graphical Abstract

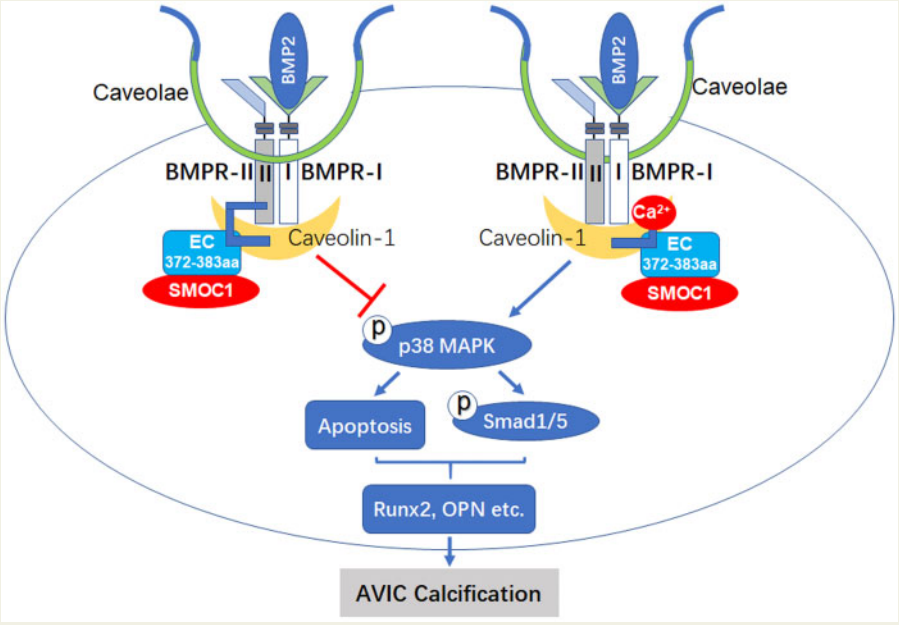

Keywords Aortic valve calcification • Aortic valve interstitial cell • SMOC1 • BMP receptor II • p38

1. Introduction

Calcific aortic valve disease (CAVD) is the most common form of heart valve disease and most common cause of aortic valve replacement in developed countries, concomitant with a rapidly increasing prevalence due to population aging.[1,2] Despite its high morbidity and high mortality, the causes and pathogenesis of CAVD remain unclear. CAVD is an active and progressive process associated with inflammation, extracellular matrix remodelling, and ectopic bone formation.[3–6] Aortic valve interstitial cells (AVICs) are the most prevalent cell type in aortic valves that are essential for valvular homeostasis and remodelling.[7] During the pathological process of CAVD, AVICs also play a major role by regulating extracellular matrix remodelling and undergoing transdifferentiation into osteoblast-like cells and calcium deposition.[8]

Bone morphogenic proteins, BMPs, which belong to the transforming growth factor-β (TGF-β) superfamily, are potent osteogenic growth factors that promote osteogenic differentiation and bone formation during development and the adult stage.[9,10] Among BMP members, BMP-2, -4, and -7 have been reported to promote the osteoblastic transdifferentiation of AVICs.[11] Furthermore, BMP2 was found to be highly expressed in calcific stenotic aortic valves and plays a critical role in aortic valve calcification.[12,13] In particular, phosphorylated Smad 1 and 5 (p-Smad1/5), which act as the main signal transducers of BMP signalling, are significantly increased in adult calcific aortic valves, suggesting the role of BMP signalling in aortic valve calcification.[14]

Secreted protein acidic and rich in cysteine (SPARC)-related modular calcium binding 1, SMOC1, is characterized as a basement membrane protein that is expressed in various tissues.[15] This protein is an extracellular glycoprotein comprising five domains—an N-terminal follistatin-like domain, two thyroglobulin-like domains, a domain unique to SMOC, and an EF-hand calcium-binding domain that is homologous to that in SPARC (also known as BM-40 and osteonectin) and is also a common structure for binding calcium ion.[15] Although the biological function of SMOC1 remains largely unknown, *Xenopus* SMOC1 protein, the orthologue of human SMOC1, acts as a BMP antagonist by inhibiting the C-terminal phosphorylation of Smad1 by affecting MAP kinase,[16] suggesting that mammalian SMOC1 may also modulate the BMP2/Smad1 signalling pathway. SMOC1 was found to be essential for ocular and limb development in humans and mice.[17–19] Moreover, SMOC1 is involved in the osteoblastic differentiation of human bone marrow-derived mesenchymal stem cells.[20] However, it remains unknown whether and, if so, how SMOC1 may regulate AVIC and aortic valve calcification.

In this study, we investigated the role of SMOC1 in AVICs and aortic valve calcification under different conditions. We found that SMOC1 inhibited warfarin or osteogenic medium induced AVIC calcification, and promoted AVIC calcification induced by high calcium/phosphate media. Mechanistically, SMOC1 directly binds to BMP receptor II (BMPRII), causing the inhibition of p38-mediated p-Smad1/5 signalling. SMOC1 loses this ability under the mutation of amino acids 372–383 of the EC domain or under high calcium conditions, leading to the promotion of AVIC calcification via increased BMPR-II expression and endocytosis.

2. Methods

2.1 Human aortic valve tissues

Human calcific aortic and mitral valve tissues were obtained from patients with rheumatic heart valve disease and chronic atrial fibrillation who had received warfarin therapy before surgical valve replacement, and from patients with non-rheumatic calcific valve disease. Non-calcific

aortic valve tissues were obtained from patients with aortic valve prolapse, aortic sinus dilatation, and aortic dissection undergoing valve replacement. Non-calcific aortic valve tissues were examined by gross examinations and microscopic examinations of haematoxylin- and eosin-stained cryosections to confirm the absence of calcification. All the studies involving human tissues were approved by the Ethics Committee of the First Affiliated Hospital of Nanjing Medical University (No. 2013-SRFA-075) and complied with the Declaration of Helsinki. All the patients signed the written informed consent before participating in the study.

2.2 Animal experiments

All the animal experiments were performed according to the protocols approved by the Ethics Committee of Nanjing Medical University for the Use and Care of Laboratory animals, and all the procedures complied with the Directive 2010/63/EU of the European Parliament on the protection of animals used for scientific purposes.

2.3 Cell culture

Primary porcine aortic valvular interstitial cells (pAVICs), human aortic valvular interstitial cells (AVICs), mitral valvular interstitial cells (MVICs), and aortic endothelial cells (AVECs) were isolated and cultured as described previously.[21,22] Briefly, aortic valves were harvested from five 2-month-old domestic pigs with mean weight of 5 kg. Pigs were sedated with Zoletil (a mixture of tiletamine and zolazepam, Virbac, France; 5 mg/kg, i.m.), and once tranquilized, a venous access was established in an ear vein. Anaesthesia was then induced using propofol (2.5 mg/kg, i.v.) from the access and maintained by isoflurane (3%, inhalation). For euthanasia, animals were given an intravenous injection of propofol (10 mg/kg, i.v.) and potassium chloride (2 M, i.v.). After a left thoracotomy was performed, the heart was quickly excised and valves were carefully dissected. pAVICs were then isolated by collagenase digestion and cultured in Dulbecco's modified Eagle's medium (Gibco, USA) supplemented with 10% foetal bovine serum (Gibco) and 1% penicillin/streptomycin. Human umbilical vein endothelial cells (HUVECs) and human dermal fibroblasts (HDFs) were kindly provided by Dr Wang. All the experiments were performed with cells at passages 3 to 5.

2.4 Transgenic mice

pH19-Tie-SMOC1-IRES/Egfp-H19 transgenic mice were generated using standard techniques.[23] PCR analysis was used to genotype mice, and the primers used were 5′-AACAGCAGCGATGACATTAACAAG-3′ and 5′-GACCCCTAGGAATGCTCGTCAA-3′. SMOC1 transgenic mice were generated in the FVB background and backcrossed into the C57BL/6J background for at least ten generations. The mice were housed in a controlled environment (20 ± 2°C, 12-h/12-h light/dark cycle) and have free access to water and diet.

2.5 Warfarin-induced AV calcification model

The mice (8-week-old males) were grouped as follows: wild-type mice with saline: $n = 6$; wild-type mice with warfarin: $n = 6$; SMOC1 transgenic mice with saline: $n = 6$; SMOC1 transgenic mice with warfarin: $n = 6$. The mice were injected with warfarin (7.57×10^{-4} mol/kg body weight; Cat. A4571; Sigma-Aldrich, USA) and vitamin K1 (5.32×10^{-5} mol/kg body weight) for 4 weeks subcutaneously under gas anaesthesia with 1.5% isoflurane. Warfarin was administered at 8 AM and 8 PM, while vitamin K1 was administered only at 8 AM. Isoflurane gas was provided at 5% to anaesthetize the mice, which were monitored during this process. Once the mice were immobile for more than 1 min, they were euthanized with 100% CO_2 inhalation.

2.6 Adenine-Vitamin-D-induced AV calcification model

The mice were separated into four groups: wild-type mice with a normal diet: $n = 6$; wild-type mice with an adenine diet: $n = 6$; SMOC1 transgenic mice with a normal diet: $n = 6$; SMOC1 transgenic mice with an adenine diet: $n = 6$. Next, 1.48×10^{-2} mol/kg of adenine (Cat. A8626; Sigma-Aldrich) was added to the diet for 3 weeks. After the evaluation of renal function by testing the serum BUN and creatinine (Cat. AU5800; Beckman Coulter, USA), vitamin D (2.27×10^{-5} mol/kg body weight; Cat. C9756; Sigma-Aldrich), dissolved in olive oil (Cat. O1514; Sigma-Aldrich), was injected intraperitoneally on 10 consecutive days under gas anaesthesia with 1.5% isoflurane. The mice were sacrificed after additional 4 days under gas anaesthesia with 5% isoflurane, followed by 100% CO_2 inhalation as above. Blood was collected, and the mice were then perfused via the left ventricle with 5 ml of PBS before tissue collection. Hearts with aortic roots were carefully dissected and embedded in optimum cutting temperature compound (OCT; Cat. 4583; Sakura, USA).

2.7 Alizarin red staining and von Kossa staining

Sections were cut at 7 μm for OCT-embedded samples. For Alizarin red staining, the 4% paraformaldehyde fixed sections were incubated with the alizarin red dye (Cat. BM1853; Bomei, China) for 3 min, followed by washing and sealing. The 4% paraformaldehyde fixed cells were stained with alizarin red solution for 1 min, and the stained cells were washed and photographed.

For von Kossa staining, the 4% paraformaldehyde fixed sections were incubated with silver nitrate solution (Cat. BM1779; Bomei) for 60 min under exposure to ultraviolet light. Next, the sections were washed with ddH_2O for 1 min and incubated with hyposulfite solution for 2 min. The sections were then stained with eosin and sealed.

2.8 Immunofluorescence staining of the aortic valve

For immunofluorescence staining, CyTM3 or Alexa-488-conjugated secondary antibody (Jackson, USA) was used after the overnight incubation of the lesions with the following primary antibodies: SMOC1 (Cat. ab155776; Abcam, USA), RUNX2 (Cat. 20700-1-AP; Proteintech, China), OPN (Cat. BS1264; Bioworld, China), p-Smad1/5/9 (Cat. 13820; Cell Signaling Technology, USA), Vimentin (Cat. ab45939, Abcam). DAPI was used to counterstain the nuclei. Digital images were acquired using a confocal laser scanning microscope (LSM 710; Carl Zeiss).

2.9 Immunohistochemistry

About 4-μm paraffin-embedded tissue sections were used for immunohistochemistry staining. Secondary antibody (Cat. 111-035-003; Jackson) conjugated with horseradish peroxidase (HRP) was used after the overnight incubation of the slides with the primary antibody SMOC1 (Cat. ab155776, Abcam) at 4°C. Next, the slides were incubated in DAB solution for 3 min and counterstained with haematoxylin for 5 min. Digital images were acquired using a microscope (Axio Imager.A2; Carl Zeiss).

2.10 TUNEL assay

Sections were cut at 4-μm for paraffin-embedded samples. Terminal deoxynucleotidyl transferase-mediated dUTP nick end labelling (TUNEL) assay was performed using DeadEnd™ Fluorometric TUNEL System (Promega, USA). Digital images were acquired using a confocal laser scanning microscope (LSM 710; Carl Zeiss).

2.11 *In vitro* pAVIC calcification

2.11.1 Warfarin-induced AVIC calcification

The warfarin-induced calcification medium contained 1.6 mmol/L of inorganic phosphate (Pi) and 10 μmol/L of warfarin (Cat. A4571; Sigma-Aldrich) as described previously.[2]

2.11.2 High-calcium/phosphate-induced AVIC calcification

To induce calcification with a high content of calcium/phosphate, the cells were cultured in medium containing 1.5 mmol/L of calcium and 2.0 mmol/L of inorganic phosphate as described previously.[24] The high calcium/phosphate media was changed every other day.

2.11.3 Osteogenic medium-induced AVIC calcification

The osteogenic differentiation of pAVICs was induced in osteogenic medium supplemented with 0.28 mmol/L of L-ascorbic acid (Cat. A4544; Sigma-Aldrich), 10 mmol/L of β-glycerophosphate (Cat. G9422; Sigma-Aldrich), 10^{-8} mmol/L of dexamethasone (Cat. 1126; Tocris, USA) and 10 ng/ml of TNF-α (Cat. 210-TA; R&D Systems, USA). The osteogenic medium was changed every 3 days.

2.12 SMOC1-plasmid construction and transfection

FLAG-tagged SMOC1 wild-type and mutant plasmids were purchased from Genechem (China). Two mutant SMOC1 plasmids were used: one was mutated from amino acids 409 to 420 (409-420aa-mut1), and the other was mutated from amino acids 372 to 383 (372-383aa-mut2). The Myc-tagged BMPR-II plasmid was also purchased from Genechem. HEK293T cells were transfected with 5 μg of expression plasmid using 10 μl of Lipofectamine® 3000 reagent (Cat. L3000-015; Invitrogen, USA) in Opti-MEM-I. The cells were incubated with the transfection mixes for 6 h, followed by replacement with DMEM/10% FBS for 72 h.

2.13 SMOC1-adenovirus vector and transduction

pAVICs were infected with recombinant adenovirus expressing human FLAG-tagged SMOC1 (Genechem) according to the manufacturer's instructions. The concentration of adenovirus SMOC1 was 3×10^7 PFU/ml. Flag-tagged mutant SMOC1 adenovirus (Ad-SMOC1-MUT) was mutated from amino acids 372 to 383, and the concentration was 1.2×10^7 PFU/ml. The efficacy of protein expression was examined by the density of adenoviral GFP.

2.14 Caveolin1-plasmid and SMOC1-adenovirus transfection assays

The caveolin1 plasmid was purchased from Genechem. HEK293T cells were transfected with 2.5 μg of the fusion plasmid using 3.75 μl of Lipofectamine® 3000 reagent (Cat. L3000-015; Invitrogen) in Opti-MEM-I. Next, the cells were infected with recombinant adenovirus expressing human FLAG-tagged SMOC1 (Genechem) according to the manufacturer's instructions. The concentration of adenovirus SMOC1 was 3×10^7 PFU/ml. Digital images were acquired using a Zeiss inverted microscope.

2.15 Inhibition of p38 signalling

p38 signalling was inhibited using the specific inhibitor SB203580 (Cat. S1076; Selleck, USA). Briefly, SB203580 (2 μmol/L per well) was added to the media containing 1.5 mmol/L of calcium and 2.0 mmol/L of inorganic phosphate.

2.16 Treatment with conditional medium from HUVECs

pAVICs were seeded on a glass-bottomed cell culture plate (Cat. 801006; NEST, China). HUVECs were cultured and transduced with SMOC1 adenovirus. After 72 h, the medium with cultured HUVECs was transferred to cultured pAVICs. This procedure was repeated for 4 days, and then the cells were fixed and blocked. FLAG and Vimentin were immunostained with FLAG (Cat. F3165; Sigma, USA) and Vimentin (Cat. ab45939; Abcam) antibodies, respectively, followed by incubation with secondary antibodies and DAPI staining. Cells were visualized using a confocal laser scanning microscope (LSM 710; Carl Zeiss).

2.17 Calcium content assay

The serum calcium content was measured using the QuantiChrom™ Calcium Assay Kit (Cat. DICA-500; BioAssay Systems, USA) according to the manufacturer's instructions. Briefly, 5 μl of serum was transferred to a 96-well plate. The working reagent (200 μl) was added per well, and the optical density was measured at 612 nm using a Synergy™ 2 Microplate Reader (BioTek, USA).

The calcium concentration was quantified colorimetrically using the o-cresolphthalein method in 0.6 mol/L of HCl extracts from cultured cells. The calcium content was normalized to the total cellular protein.

2.18 Alkaline phosphatase activity assay

Alkaline phosphatase (ALP) activity was measured using the ALP LabAssay™ (Cat. 291-58601; Wako Chemicals GmbH, Japan) according to the manufacturer's instructions. The cell layers were lysed in 250 μl of ice-cold 0.05% Triton X-100 in PBS, frozen and thawed three times. Next, the cell lysates were collected and mixed with 100 μl of buffer solution, followed by incubating for 15 min at 37°C. After adding 80 μl of stop solution, the optical density of each well was measured at 405 nm. ALP activity (U; μmol of p-nitrophenylphosphate released/min) was normalized to the total cellular protein.

2.19 Immunoprecipitation and Western blot analysis

For immunoprecipitation, the samples were collected and lysed in 50 mmol/L of Tris-HCl (pH 7.4) lysis buffer. The supernatant was immunoprecipitated with 5 μg of anti-BMPR-II (Cat. sc-393304; Santa Cruz, USA), anti-FLAG (Cat. F3165; Sigma), anti-Myc (Cat. 05-724; Millipore, USA) or anti-SMOC1 (Cat. ab155776; Abcam) overnight accordingly and then was incubated with Dynabeads™ Protein A (Cat. 1002 D, Invitrogen) for another 3 h at 4°C. Next, the cell lysates were subjected to western blot analysis as described previously.[2] The primary antibodies used were SMOC1 (Cat. ab155776; Abcam), RUNX2 (Cat. 12556; Cell Signaling Technology), BMP2 (Cat. ab14933; Abcam), p-Smad1/5 (Cat. 9516; Cell Signaling Technology), Smad1 (Cat. 6944; Cell Signaling Technology), p-p38 (Cat. 4511; Cell Signaling Technology), p38 (Cat.

9212; Cell Signaling Technology), Caspase-3 (Cat. 9662; Cell Signaling Technology), BMPR-II (Cat. sc-393304; Santa Cruz), FLAG (Cat. F3165; Sigma) and Myc (Cat. 05-724; Millipore). Image Lab™ software was used to quantify the band density.

2.20 SMOC1 endocytosis assay

pAVICs were seeded in 6-well culture plates and then were cultured to 90% confluency, followed by treatment with recombinant human SMOC1 protein (200 ng/ml and 400 ng/ml; Cat.6074-SM; R&D Systems) for 6 h. Next, cell lysates were prepared and subjected to western blot analysis as described previously.[2] The primary antibody used was SMOC1 (Cat. ab155776; Abcam), and Image Lab™ software was used to quantify the band density.

2.21 In-cell co-immunoprecipitation

In-cell co-immunoprecipitation was performed using the Duolink® In Situ PLA® Probe (Cat. DUO92004; Sigma) following the manufacturer's instructions. Briefly, the cells were blocked and incubated with anti-Vimentin (Cat. ab45939; Abcam) overnight at 4°C. Next, the cells were incubated with anti-BMPR-II (Cat. sc-393304; Santa Cruz) and anti-FLAG (F7425; Sigma) antibodies for 2 h at room temperature, followed by incubation with anti-rabbit plus and anti-mouse minus PLA® probes for 60 min at 37°C. Ligase was added to the cells, followed by incubation for 30 min at 37°C. The fluorescence signal was then amplified by the addition of polymerase for 100 min at 37°C. The in-cell complexes were visualized by confocal microscopy (LSM 710; Carl Zeiss).

2.22 RNA extraction, RT–PCR, and real-time PCR

Total RNA was extracted from the cells using TRI Reagent® (Cat. T9424; Sigma), and 500 ng of RNA was reverse-transcribed into cDNA using the PrimeScript™ RT Master Mix (Cat. RR036A; Takara, Japan). Real-time PCR was performed using the ABI Prism 7900 system. PCR amplification was performed using the following Taqman probes: BMP2(sus): 5′-AGTTCGCGGCGTCTACTG-3′, 5′-CAACTCAAACTC GCTGAGGA; RUNX2(sus): 5′-CTTTTGGGATCCGAGCAC-3′, 5′-GGCTCACGTCGCTCATCT-3′; OPN(sus): 5′-AATCTAAGAAGTTC CGCAGATCC-3′, 5′-CCACATGTGACGTGAGGTCT-3′ and GAP DH(sus): 5′-ACAGACAGCCGTGTGTTCC-3′, 5′-ACCTTCACCATC GTGTCTCA-3′, which was served as internal calibrator. The primers of RT–PCR reactions are SMOC1(human): 5′-TCTAAGCCGACACCC ACG-3′, 5′-GCTCTGAGAACCTCCCACCT-3′; GAPDH(human): 5′-ATGACATCAAGAAGGTGGTG-3′, 5′-CATACCAGGAAATGAGCT TG-3′; GAPDH(sus): 5′-ACCACAGTCCATGCCATCAC-3′, 5′-TCC ACCACCCTGTTGCTGTA-3′; BMP4(sus): 5′-TCGTTACCTCAAGG GAGTGG-3′, 5′-GGAGCCACAATCCAGTCATT-3′; BMP7(sus): 5′-GCTATGCCGCCTACTACTGC-3′, 5′-GTTGGAGCTGTCGTCGAA GT-3′; BMP9(sus): 5′-GGCTCAGGACCCAACCTAA-3′, 5′-AGGAT GGCGCTGTTGGAT-3′; BMP2(human): 5′-TGCAGGAAAGTGAATG ATGG-3′, 5′-TGATGAGGGCCACGAGATA-3′; BMP4(human): 5′-CTTTACCGGCTTCAGTCTGG-3′, 5′-GGGATGCTGCTGAGGTTA AA-3′; BMP7(human): 5′-CTCCATTGCTCGCCTTG-3′, 5′-GGATGC TGCCACTGAAAA-3′; BMP9(human): 5′-CCCAGGACATTCAGGA TGAG-3′, 5′-CTGCTGTGGTCATTGGAGAA-3′. The RT–PCR products were analysed by agarose gel electrophoresis.

2.23 MTT assay

pAVICs were seeded with 2,000 cells/well in a 96-well plate. After 24 or 48 h of calcifying medium treatment, 10 μL of MTT solution (Cat. C0009; Beyotime, China) was added per well, followed by incubation for 4 h at 37°C. Next, 100 μL of formazan solvent was added per well to dissolve the formazan crystals. The absorbance at 570 nm was measured using a Synergy™ 2 Microplate Reader (BioTek).

2.24 Flow cytometry

To induce apoptosis, pAVICs were starved for 7 days. The cells were then incubated with phycoerythrin (PE)-conjugated propidium iodide (PI) and allophycocyanin (APC)-conjugated Annexin-V (Fcmacs Biotech Co. Ltd., China) in binding buffer for 15 min at room temperature according to the manufacturer's instructions. Cells were washed and sorted using a FACSCalibur instrument (BD Biosciences, USA) within 1 h of staining.

To determine the role of SMOC1 in calcification-induced cell apoptosis, the cells were treated with media containing 1.5 mmol/L of calcium and 2.0 mmol/L inorganic phosphate, and the extent of cell apoptosis was assayed as above.

2.25 Real-time analysis of cell growth

pAVICs were plated in 16-well E-plates at a concentration of 4,000 cells/well and were transduced with adenovirus when the cells were cultured to 60%–70% confluency. The impedance-based growth was monitored continuously using the xCELLigence RTCA TP System (ACEA Biosciences Inc., USA).

2.26 Statistical analysis

Quantitative values were expressed as means ± standard error of the mean (SEM) and represented data from at least three independent experiments. After confirming that all the variables were normally distributed by the Kolmogorov–Smirnov test followed by Q–Q plot analysis, significant differences were determined by Student's *t*-test or the Mann–Whitney *U* test for comparison between two groups and ANOVA followed by Bonferroni's multiple comparison test for comparison among three or more groups. *P* values less than 0.05 were considered statistically significant. All the statistical calculations were performed using GraphPad Prism 5.0 (GraphPad Software).

3. Results

3.1 SMOC1 expression and cellular localization in human aortic valves

We first examined the expression levels of SMOC1 in human calcific and non-calcific aortic valves. Immunostaining demonstrated that SMOC1 was mainly located in the endothelial and sub-endothelial layers in non-calcific aortic valves. The intensity of SMOC1 in the sub-endothelial layer was lower in calcific aortic valves than in non-calcific aortic valves, and SMOC1 located in the interstitial cell area was mainly found in calcific aortic valves (*Figure 1A*). The distribution of SMOC1 was similar in both rheumatic and non-rheumatic calcified valves (Supplementary material online, *Figure S1*). Western blotting also showed that the total SMOC1 levels were lower in calcific aortic valves than in non-calcific aortic valves (*Figure 1B*). Because SMOC1 is a secreted protein,[15] we examined the intrinsic expression of SMOC1 in valve endothelial cells, valve interstitial

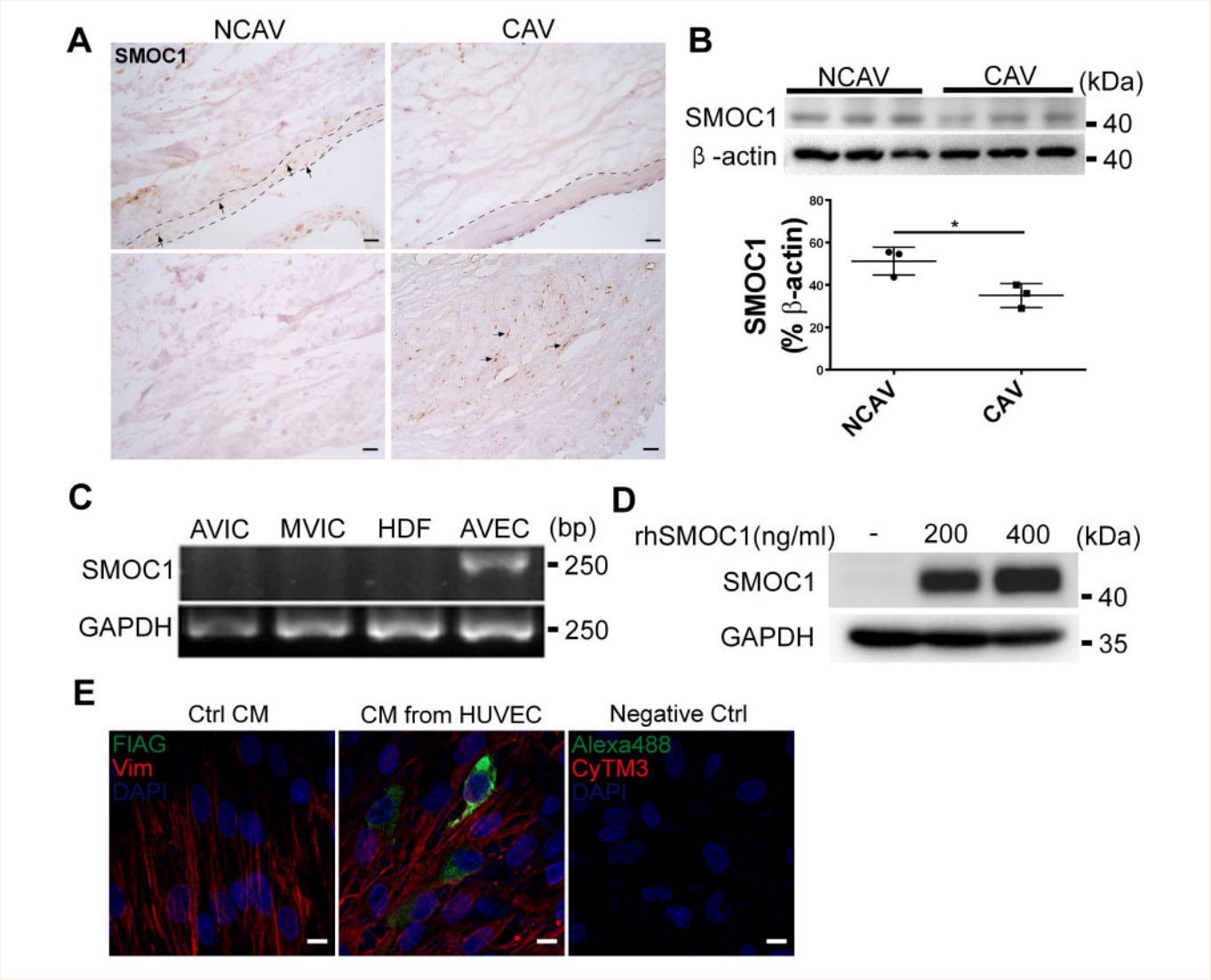

Figure 1 SMOC1 is expressed by aortic valve endothelial cells and secreted into aortic valve interstitial cells. (*A*) Representative immunohistochemistry staining of calcific ($n = 3$) and non-calcific human aortic valves ($n = 3$) with the indicated antibodies (Scale bar: 50 μm; NCAV: non-calcific human aortic valve; CAV: calcific human aortic valve). (*B*) The protein levels of SMOC1 were assessed by western blotting in calcific ($n = 3$) and non-calcific human aortic valves ($n = 3$). The SMOC1 levels were quantified by normalizing to the β-actin levels. The data are shown as the means ± SEM. *$P < 0.05$, unpaired *t*-test. (*C*) RT–PCR demonstrated that SMOC1 is specifically expressed by endothelial cells, not valve interstitial cells, including AVICs and MVICs, or human dermal fibroblast (HDF) cells ($n = 3$). (*D*) The entrance of exogenous SMOC1 into pAVIC cytoplasm was assessed by western blotting. pAVICs were treated with different doses of recombinant SMOC1, and then cytoplasmic proteins were extracted for western blotting ($n = 3$). (*E*) Porcine AVICs (pAVICs) were treated with conditioned medium from HUVECs transfected with Ad-SMOC1, and then SMOC1 secreted into pAVICs was immunostained with anti-flag antibody (Scale bar: 20 μm; $n = 6$). The data are shown as the means ± SEM of triplicates and represent one of three experiments performed.

cells, and fibroblasts. We found that SMOC1 was solely expressed by aortic valve endothelial cells, not AVICs or fibroblasts (*Figure 1C*). Because SMOC1 can be found away from endothelial cells in human calcific aortic valves, we hypothesized that secreted SMOC1 is involved in aortic valve and AVIC calcification. To confirm whether secreted SMOC1 can enter AVICs, we treated cultured porcine AVICs (pAVICs) with recombinant SMOC1, and the assay of cytoplasmic protein showed that SMOC1 was absorbed by pAVICs (*Figure 1D*). We further treated pAVICs with conditioned media from HUVECs transfected with the FLAG-tagged SMOC1 adenovirus vector, and immunofluorescence staining showed that secreted FLAG-tagged SMOC1 was detected in pAVICs (*Figure 1E*). Next, we examined the effects of SMOC1 on pAVIC proliferation and apoptosis. The overexpression of SMOC1 showed no effect on pAVIC proliferation (Supplementary material online, *Figure S2A*), but increased serum starvation-induced cell apoptosis (Supplementary material online, *Figure S2B* and *C*).

3.2 Overexpression of SMOC1 inhibits warfarin and osteogenic medium-induced calcification but promotes high-calcium-medium-induced calcification in PAVICs

To determine the effect of SMOC1 on AVIC and AV calcification, we first studied the effect of SMOC1 on our previously reported warfarin

calcification model.[22] We found that the overexpression of SMOC1 inhibited pAVIC calcium deposition (*Figure 2A and B*) and alkaline phosphatase (ALP) activity (*Figure 2C*) and decreased the protein levels of osteogenic markers, including RUNX2 and BMP2 (*Figure 2D–F*). To further confirm the *in vitro* results, we generated a transgenic mouse model specifically expressing SMOC1 in endothelial cells (Supplementary material online, *Figures S3A–D* and *S4A–E*) and induced AV calcification with warfarin as we previously reported.[22] Both alizarin red and von Kossa staining showed less calcium deposition in SMOC1 transgenic mice than in wild-type (WT) mice (*Figure 2G and H*, and Supplementary material online, *Figure 5A and B*). Consistent with decreased calcium deposition, SMOC1 transgenic mice showed much lower expression of osteogenic marker genes, including RUNX2 and OPN, in aortic valves compared with WT mice, as indicated by immunofluorescence staining (*Figure 2G and H*).

To further confirm the effect of SMOC1 on calcification in pAVICs, we examined the other two recognized calcification models. In the osteogenic medium (OM)-treated model, overexpression of SMOC1 still inhibited pAVIC calcification (Supplementary material online, *Figure S6 A–C*). However, in the high-calcium/phosphate-medium-treated model, overexpression of SMOC1 increased pAVIC calcification (*Figure 3A–F*, and Supplementary material online, *Table S1*). With the increase level of extracellular calcium concentration, the influence of SMOC1 on pAVIC calcification became more and more obvious, and a significant difference was observed when 0.75 mM calcium was added into media. Moreover, increasing extracellular calcium concentration did not affect the uptake of recombinant SMOC1 by pAVICs (Supplementary material online, *Figure S7 A–D*). Next, we further confirmed the opposite effect of SMOC1 on high-calcium/phosphate-medium-induced AV calcification in the renal-dysfunction-plus-vitamin D-induced AV calcification model. Renal dysfunction was induced by the adenine diet for three weeks, and then the serum creatinine and blood urea nitrogen levels were examined (Supplementary material online, *Figure S8A*). Next, vitamin D was injected to generate the high-calcium-induced aortic valve calcification model. Vitamin D, but not warfarin treatment, increased the serum calcium content (Supplementary material online, *Figure S9A* and *B*). No significant difference was found in the renal function between SMOC1 transgenic mice and WT mice treated with adenine and Vitamin D (Supplementary material online, *Figure S8B*). Alizarin red staining showed that calcium deposition significantly increased in the aortic valves of SMOC1 transgenic mice compared with that in WT mice (*Figure 3G and H*, and Supplementary material online, *Figure S10A* and *B*). Moreover, immunofluorescence staining showed that the levels of RUNX2 and OPN were significantly elevated in the aortic valves of SMOC1 transgenic mice (*Figure 3G and H*). These results suggest that SMOC1 inhibits aortic valve calcification under normal extracellular calcium conditions but increases aortic valve calcification under high extracellular calcium conditions.

3.3 Inhibition of BMP2 signalling by SMOC1 depends on a normal extracellular calcium condition

BMP2 signalling was negatively regulated by *Xenopus* SMOC1.[16] To confirm the effects of SMOC1 on BMP2 signalling in pAVICs, we treated pAVICs with recombinant human BMP2 (rhBMP2). Western blotting demonstrated that SMOC1 inhibited the downstream targets of BMP2 signalling, including p-Smad1/5 and RUNX2 (Supplementary material online, *Figure S11A* and *B*). Similar to the results of rhBMP2, overexpression of SMOC1 decreased the levels of p-Smad1/5 in warfarin- or OM-treated pAVICs (*Figure 4A* and Supplementary material online, *Figure S6C*). By contrast, SMOC1 increased p-Smad1/5 in high-calcium/phosphate-medium-treated pAVICs (*Figure 4B*). To further confirm the *in vitro* results, we measured the levels of p-Smad1/5 in warfarin- and vitamin D-induced aortic valve calcification models. Consistent with the *in vitro* results, the levels of p-Smad1/5 were decreased in SMOC1 transgenic mice treated with warfarin but increased in SMOC1 transgenic mice treated with vitamin D compared with WT mice (*Figure 4C–E*). To exclude the effects of endothelial cell synthesized BMPs on p-Smad1/5 in high calcium/phosphate condition, we examined BMP2, BMP4, BMP7, and BMP9 expression in HUVECs and found that overexpression of SMOC1 decreased BMP2 expression and did not affect BMP4, 7, 9 expressions in HUVECs under high calcium/phosphate condition (Supplementary material online, *Figure S12 A–D*). In pAVICs, overexpression of SMOC1 decreased the BMP4 mRNA levels and did not affect BMP9 expression in high calcium/phosphate condition (Supplementary material online, *Figure S13 A–C*). These results indicated that other BMPs mentioned above were not associated with the effects of SMOC1 under high calcium/phosphate status.

3.4 p38 is a key factor for the dual effects of SMOC1 on AV calcification

BMP2 signalling can be transduced by the activation of the p38 MAPK pathway.[25] To determine why SMOC1 showed opposite effects on calcification under the high calcium/phosphate condition, we examined the effect of SMOC1 on pAVIC apoptosis under the high calcium/phosphate condition and the levels of phosphorylated p38 (p-p38) in pAVICs treated with different media. The overexpression of SMOC1 increased cell apoptosis and the p-p38 levels in the high calcium/phosphate model (*Figure 5A* and Supplementary material online, *Figure S14A–D*) but decreased the p-p38 levels in non-high-calcium media with the addition of warfarin, OM, and rhBMP2 (*Figure 5B–D*). High phosphate is a pro-apoptotic factor, but the phosphate levels in the warfarin group were comparable to those in the high calcium/phosphate group (Supplementary material online, *Table S1*). We also used the MTT assay to compare the cell toxicity of different medium, and no difference was found in the cell viability between the control and SMOC1 overexpression group under calcifying medium treatment (Supplementary material online, *Figure S15A* and *B*). Our data suggest that p-p38 may act as an important mediator for SMOC1-enhanced pAVIC calcification. We examined whether the inhibition of p38 activation could rescue the effects of SMOC1 under the high calcium/phosphate condition. The suppression of p-p38 by the specific inhibitor SB203580 (*Figure 5E*) significantly blunted the enhanced calcium deposition and osteogenic marker gene expression in SMOC1-overexpressed pAVICs treated with high calcium/phosphate media (*Figure 5F–H*, and Supplementary material online, *Figure S16A* and *B*). Western blot analysis demonstrated that the inhibition of p-p38 blunted the elevation of p-Smad1/5 (*Figure 5I*) and cleaved caspase-3 (Supplementary material online, *Figure S16C* and *D*). These results suggest that SMOC1 promotes high-calcium/phosphate-induced pAVIC calcification by increasing p-p38 mediated p-Smad1/5 signalling.

3.5 SMOC1 inhibits BMP2 signalling by directly binding to BMPR-II with amino acids 372–383

To further explore the mechanism underlying how SMOC1 regulates p38-mediated BMP2 signalling transduction, we first examined whether

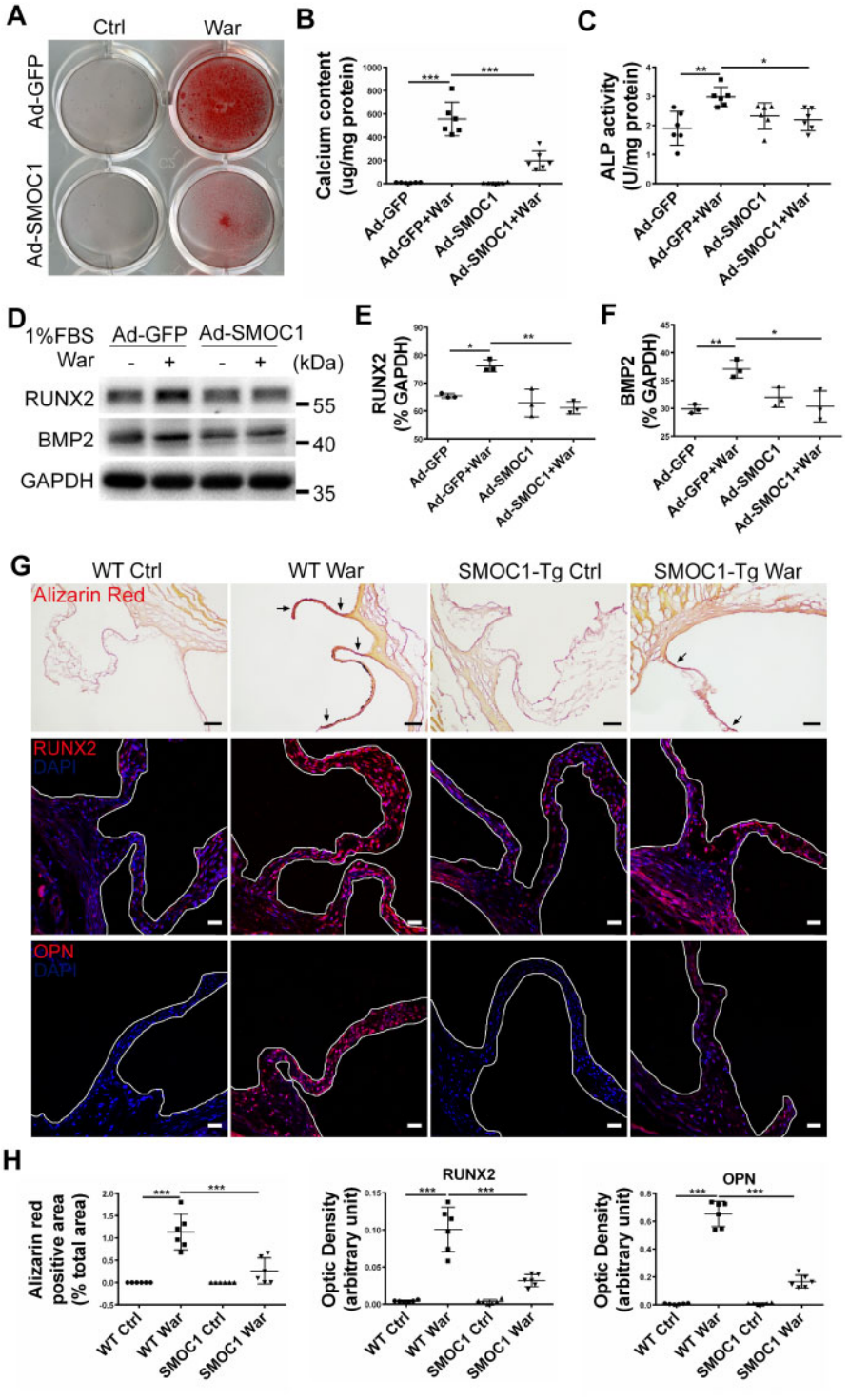

Figure 2 Overexpression of SMOC1 inhibits warfarin-induced AV calcification *in vitro* and *in vivo*. (*A–C*) Calcium deposition in pAVICs was determined by alizarin red staining [*A*] and calcium content measurement [*B*]. Alkaline phosphatase (ALP) activity was measured using the LabAssay^{TM} ALP kit [*C*] ($n = 6$ per experiment). (*D–F*) The expression levels of RUNX2 and BMP2 were assessed by western blotting. The RUNX2 and BMP2 levels were quantified by normalizing to the GAPDH levels ($n = 3$) [*E, F*]. (*G*) Wild-type and SMOC1 transgenic mice were injected with warfarin for 4 weeks. Representative images of alizarin red staining show calcium deposition in aortic valves. Osteogenic markers, including RUNX2 and OPN, were stained with the indicated immunofluorescent antibodies. (*H*) The intensity of immunostaining was assessed using ImageJ software. SMOC1 transgenic mice showed decreased alizarin red, RUNX2, and OPN staining in the calcific areas of aortic valves compared with wild-type mice after warfarin treatment (Scale bar: 50 μm; $n = 6$ per group). The data are shown as the means ± SEM of triplicates and are representative of one of three experiments performed. *$P < 0.05$, **$P < 0.01$, ***$P < 0.001$, ANOVA followed by Bonferroni's multiple comparison test.

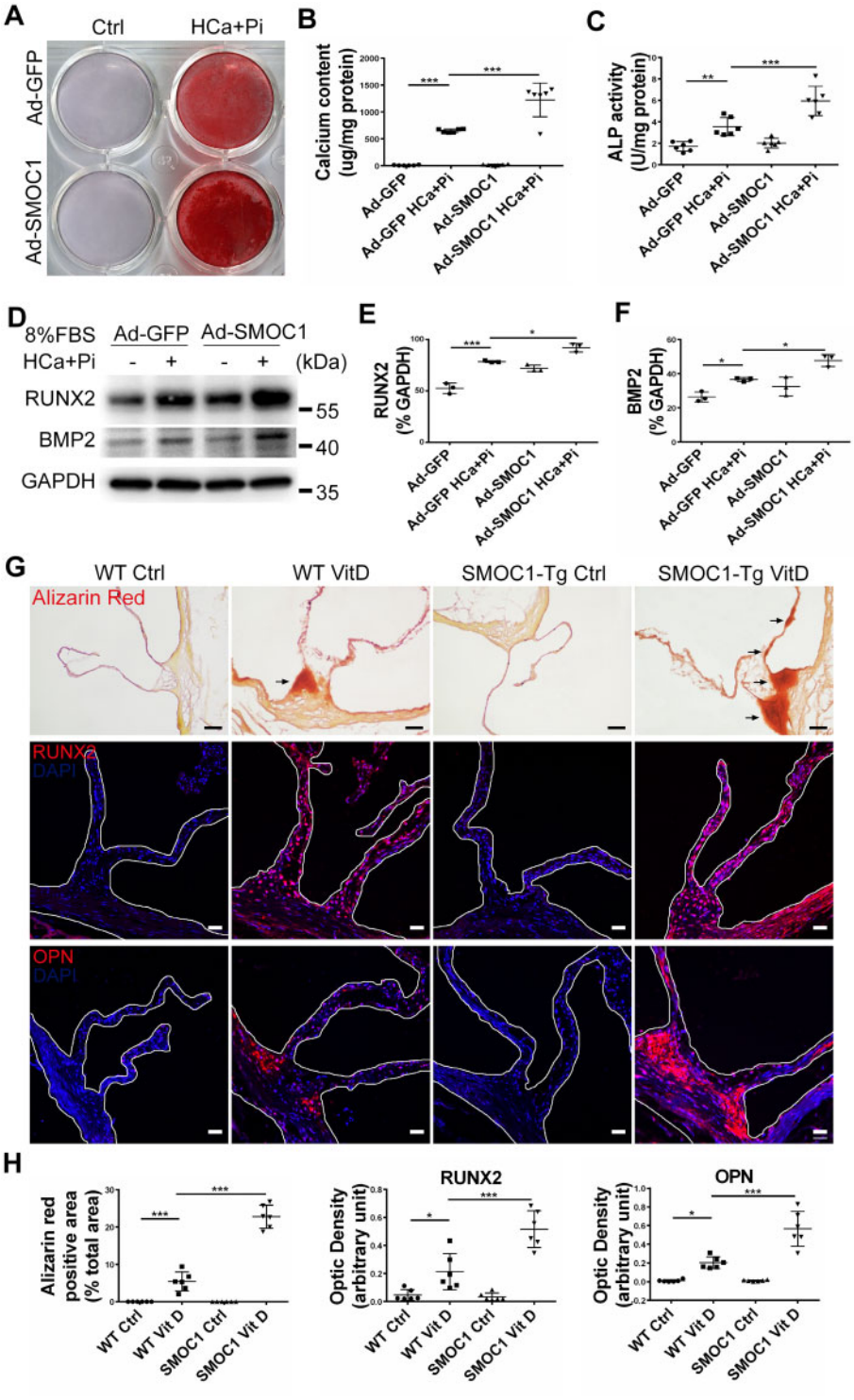

Figure 3 Overexpression of SMOC1 promotes high extracellular-calcium-induced AV calcification *in vitro* and *in vivo*. (*A–C*) Calcium deposition in pAVICs was determined by alizarin red staining [*A*] and calcium content measurement [*B*]. Alkaline phosphatase (ALP) activity was determined and measured by the LabAssay™ ALP kit [***C***] ($n = 6$ per experiment). (*D–F*) The expression levels of RUNX2 and BMP2 were assessed by western blotting. The RUNX2 and BMP2 levels were quantified by normalizing to the GAPDH levels ($n = 3$) [*E, F*]. (*G*) Wild-type and SMOC1 transgenic mice were injected with vitamin D after an adenine diet for 10 days. Representative images of alizarin red staining show calcium deposition in aortic valves. Osteogenic markers, including RUNX2 and OPN, were stained with the indicated immunofluorescent antibodies. (*H*) The intensity of immunostaining was assessed using ImageJ software. SMOC1 transgenic mice showed increased alizarin red, RUNX2, and OPN staining in the calcific areas of aortic valves compared with wild-type mice after vitamin D treatment (Scale bar: 50 μm; $n = 6$ per group). The data are shown as the means ± SEM of triplicates and are representative of one of three experiments performed. *$P < 0.05$, **$P < 0.01$, ***$P < 0.001$, ANOVA followed by Bonferroni's multiple comparison test.

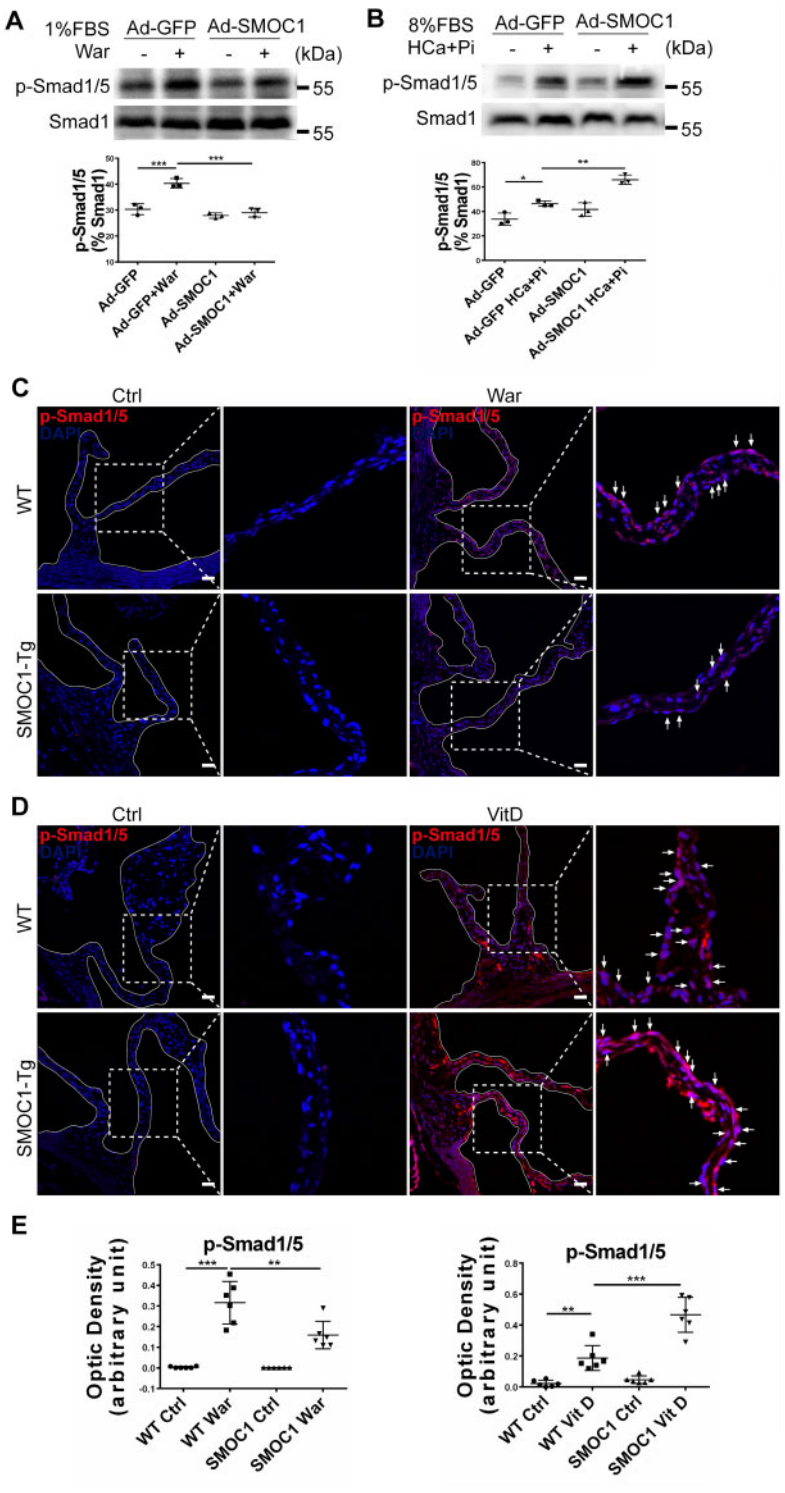

Figure 4 SMOC1 dually regulates the phosphorylation of smad1/5 under different extracellular calcium conditions. (*A*) The expression levels of p-Smad1/5 and Smad1/5 in warfarin-induced pAVIC calcification model were assessed by western blotting. The p-Smad1/5 levels were quantified by normalizing to the Smad1/5 levels ($n = 3$). (*B*) The expression levels of p-Smad1/5 and Smad1/5 in the high-calcium/phosphate -medium-induced pAVIC calcification model were assessed by western blotting. The p-Smad1/5 levels were quantified by normalizing to the Smad1/5 levels ($n = 3$). (*C* and *D*) Representative immunofluorescence staining of warfarin- or vitamin D-induced calcific aortic valves with the indicated antibodies. (*E*) Quantification of the intensity of immunostaining. SMOC1 transgenic mice show a lower intensity of p-Smad1/5 staining in warfarin-treated aortic valves but higher intensity of p-Smad1/5 staining in vitamin D-treated aortic valves than wild-type mice (Scale bar: 50 μm; $n = 6$ per group). The data are shown as the means ± SEM of triplicates and are representative of one of three experiments performed. $^{*}P < 0.05$, $^{**}P < 0.01$, $^{***}P < 0.001$, ANOVA followed by Bonferroni's multiple comparison test.

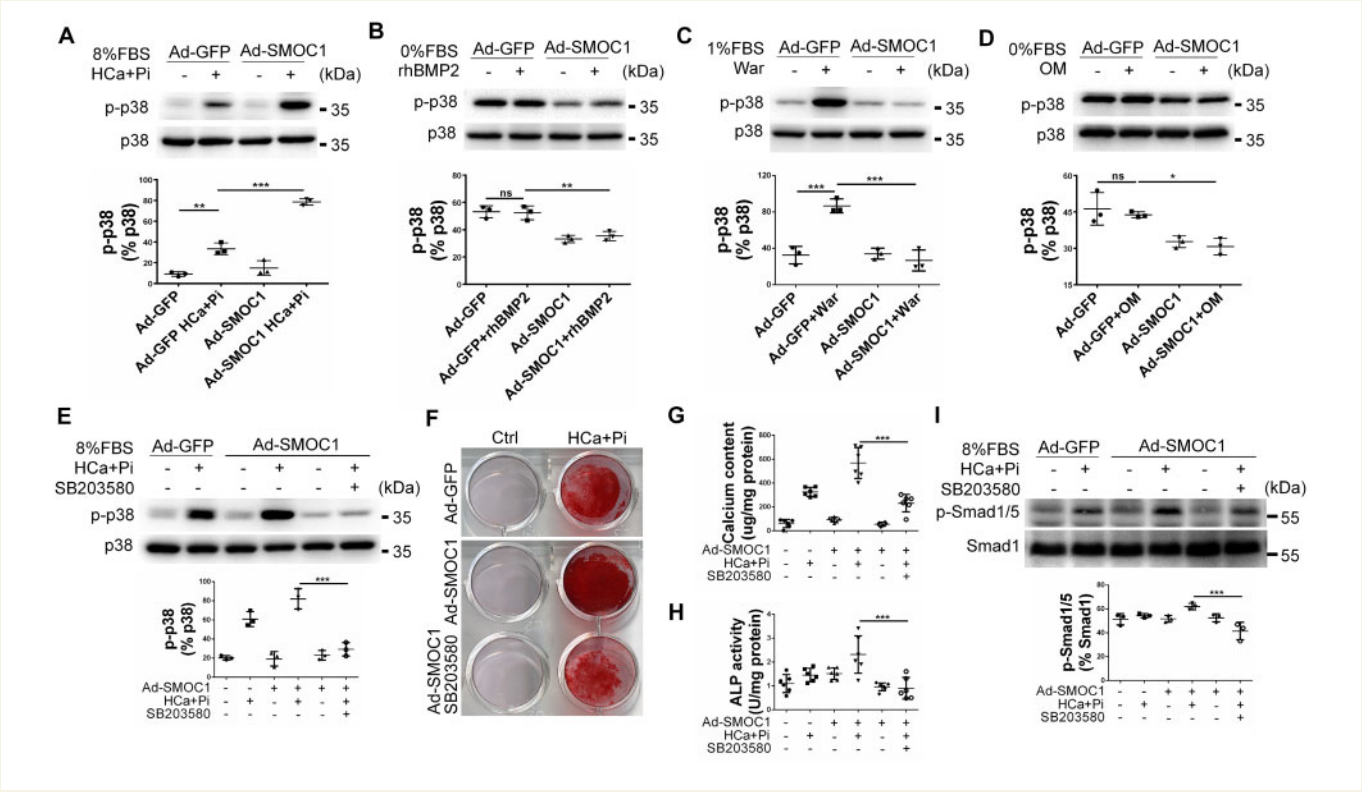

Figure 5 P38 is a key mediator for the dual effects of SMOC1 on AV calcification. (*A*) The expression levels of p-p38 and p38 in the high-calcium/phosphate-medium-induced pAVIC calcification model were assessed by western blotting. The p-p38 levels were quantified by normalizing to the p38 levels ($n = 3$). (*B*) The expression levels of p-p38 and p38 in the warfarin-induced pAVIC calcification model were assessed by western blotting. The p-p38 levels were quantified by normalizing to the p38 levels ($n = 3$). (*C*) The expression levels of p-p38 and p38 in the OM-induced pAVIC calcification model were assessed by western blotting. The p-p38 levels were quantified by normalizing to the p38 levels ($n = 3$). (*D*) The expression levels of p-p38 and p38 in rhBMP2-treated pAVICs were assessed by western blotting. For quantification, the p-p38 level was normalized to that of p38 ($n = 3$). (*E*) The expression levels of p-p38 and p38 were assessed by western blotting. The p-p38 levels were quantified by normalizing to the p38 levels ($n = 3$). (*F–H*) Calcium deposition was determined by alizarin red staining [*F*] and calcium content measurement [*G*], and alkaline phosphatase (ALP) activity was determined using the LabAssay™ ALP kit [*H*] ($n = 6$ per experiment). (*I*) The expression levels of p-Smad1/5 and Smad1 were assessed by western blotting. The p-Smad1/5 levels were quantified by normalizing to the Smad1 levels ($n = 3$). The data are shown as the means ± SEM of triplicates and are representative of one of three experiments performed. ns: $P > 0.05$, $^{*}P < 0.05$, $^{**}P < 0.01$, $^{***}P < 0.001$, ANOVA followed by Bonferroni's multiple comparison test.

an interaction occurred between SMOC1 and BMP receptors. Co-immunoprecipitation and the Duolink® proximity ligation assay by either BMP receptor II (BMPR-II) or FLAG antibodies showed that SMOC1 directly bound to BMPR-II in pAVICs treated with rhBMP2 in the absence of high extracellular calcium (*Figure 6A and B*). Considering that the high content of calcium played an important role in the dual effects of SMOC1, we proposed that the extracellular calcium-binding (EC) domain might be the key region of SMOC1 to interact with BMPR-II. We generated two plasmid vectors containing the mutant EC domain of SMOC1 with different sites, including the mutations of amino acids 372–383 or 409–420. Co-immunoprecipitation in co-transfected 293 T cells with mutant SMOC1 and BMPR-II showed that the interaction between SMOC1 and BMPR-II depended on the motif of amino acids 372–383 (*Figure 6C*). To confirm whether amino acids 372–383 contributed to the SMOC1-mediated suppression of BMP2 signalling, we generated a mutant SMOC1 adenovirus vector with the mutation of amino acids 372–383 (Supplementary material online, *Figure S17*). Co-immunoprecipitation showed that pAVICs transfected with mutant SMOC1 lost the ability to bind to BMPR-II (*Figure 6D*). Additionally, overexpression of mutant SMOC1 lost the ability to suppress p-p38 and the downstream targets of BMP2 signalling (*Figure 6E–H*). These results suggest that the motif containing amino acids 372–383 of SMOC1 is essential for the biological effects of SMOC1.

3.6 SMOC1 increases BMPR-II expression and promotes endocytosis under high extracellular calcium conditions

To explore why SMOC1 enhanced p-p38 under high calcium conditions, we examined the binding rate of BMP2 with BMPR-II using crosslinked membrane protein and found that SMOC1 did not increase the ability of BMP2 binding to BMPR-II (*Figure 7A and B*), suggesting that SMOC1 does not affect BMP2-induced direct p-Smad1/5 under high calcium condition. Next, we examined the protein levels of BMPR-II under high calcium and normal calcium conditions. We found that the increased BMPR-II was only found under high extracellular calcium conditions, and the overexpression of SMOC1 further increased the levels of BMPR-II (*Figure 7C and D*). Because the activation of Smad1/5 mediated by p-p38 depends on caveolin-1-mediated endocytosis of the BMPR complex,[26] we co-transfected pAVICs with caveolin-1 and SMOC1, and then treated

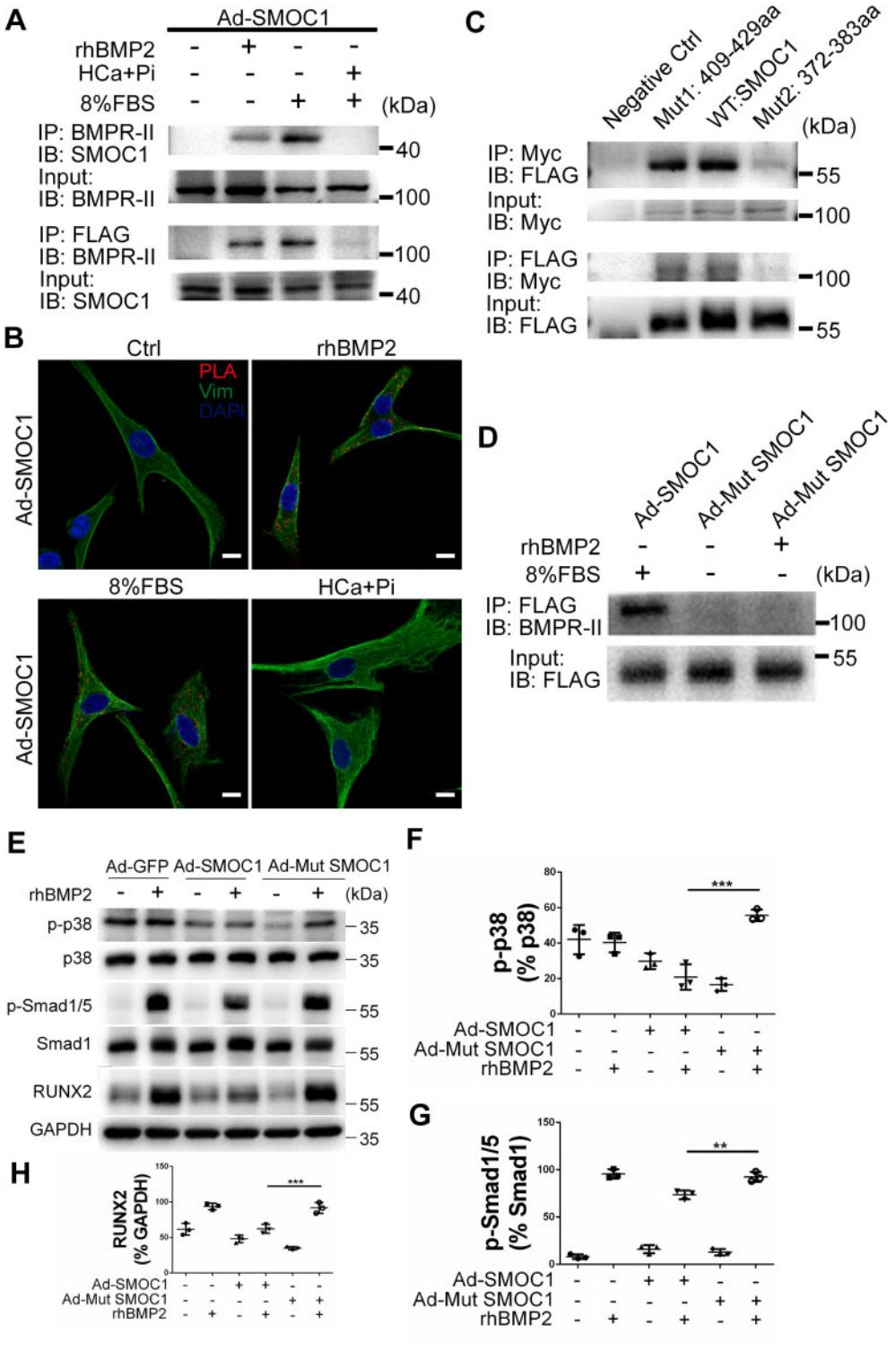

Figure 6 Amino acids 372–383 are the binding region of SMOC1 for BMPR-II and are essential for the regulation of BMP2 signal transduction. (*A*) The direct interaction between SMOC1 and BMPR-II was determined by co-immunoprecipitation with the indicated antibodies ($n = 3$). (*B*) In situ binding of SMOC1 and BMPR-II was visualized using the Proximity Ligation Assay in pAVICs and FLAG and BMPR-II primary antibodies. Red spots indicate interactions between SMOC1 and BMPR-II (Scale bar: 20 μm; $n = 3$). (*C*) Myc-tagged BMPR-II and FLAG-tagged wild-type SMOC1 or the regional mutants of SMOC1 were transfected into pAVICs. The binding of mutants SMOC1 and BMPR-II was determined by co-immunoprecipitation with the indicated antibodies ($n = 3$). (*D*) The interaction between BMPR-II and mutant SMOC1 with the mutation of amino acids 372–383 was assessed by co-immunoprecipitation ($n = 3$). (*E*) The expression levels of p-Smad1/5, Smad1, p-p38, p38, and RUNX2 were assessed by western blotting. (*F–H*) The p-Smad1/5, p-p38, and RUNX2 levels were quantified by normalizing to the Smad1, p38, and GAPDH levels, respectively ($n = 3$). The data are shown as the means ± SEM of triplicates and are representative of one of three experiments performed. $^{**}P < 0.01$, $^{***}P < 0.001$, ANOVA followed by Bonferroni's multiple comparison test.

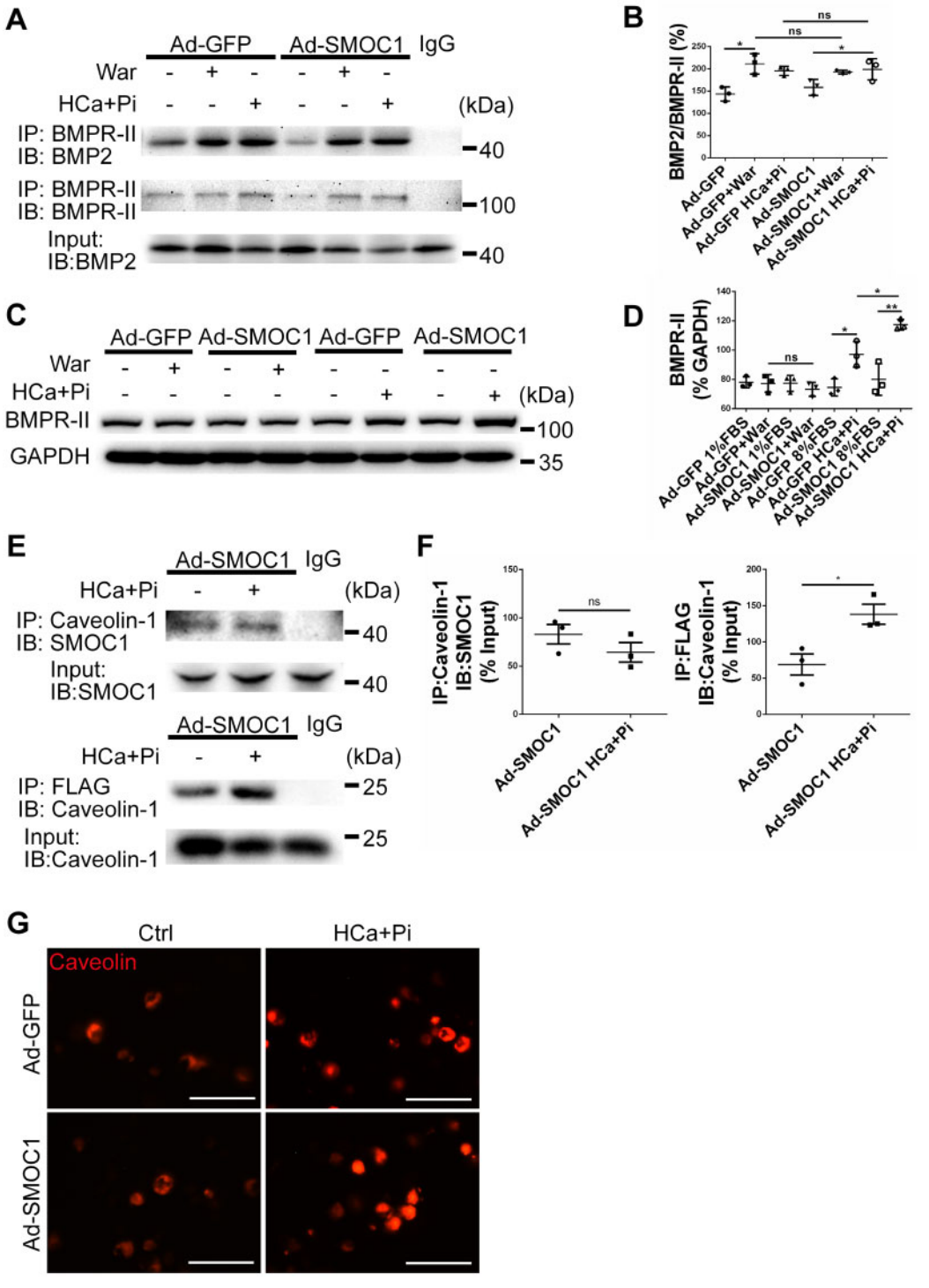

Figure 7 SMOC1 promotes high extracellular calcium-induced AVIC calcification by increasing BMPR-II expression and endocytosis. (*A* and *B*) The binding ability of BMP2 to BMPR-II was assessed by co-immunoprecipitation after specific crosslinker (BS3) treatment. The binding of BMP2 was quantified by normalizing to precipitated BMPR-II [*B*] ($n = 3$). The data are shown as the means ± SEM of triplicates and are representative of one of three experiments performed. ns: $P > 0.05$, $^{*}P < 0.05$, ANOVA followed by Bonferroni's multiple comparison test. (*C* and *D*) The expression levels of BMPR-II after different treatments were assessed by western blotting and normalized to the GAPDH levels [*D*] ($n = 3$). The data are shown as the means ± SEM of triplicates and are representative of one of three experiments performed. ns: $P > 0.05$, $^{*}P < 0.05$, $^{**}P < 0.01$, ANOVA followed by Bonferroni's multiple comparison test. (*E* and *F*) The direct interaction between SMOC1 and caveolin-1 was determined by co-immunoprecipitation with the indicated antibodies. The interaction between SMOC1 and caveolin-1 was quantified by normalizing to precipitated SMOC1 and caveolin-1 [*F*] ($n = 3$). The data are shown as the means ± SEM of triplicates and are representative of one of three experiments performed. ns: $P > 0.05$, $^{*}P < 0.05$, unpaired *t*-test. (*G*) Endocytosis of pAVICs under different treatments was assessed by immunostaining of caveolin-1 with the indicated antibody (Scale bar: 50 μm; $n = 3$).

pAVICs with high calcium/phosphate medium. We found that high calcium did not affect the interaction between SMOC1 and caveolin-1 and enhanced the endocytosis of pAVICs (*Figure 7E–G*). We also measured the expression levels of SMOC1 under the warfarin and high calcium conditions and found that both warfarin and high calcium/phosphate medium increased the cellular levels of SMOC1. However, the intracellular levels of SMOC1 in the high calcium/phosphate group was lower than that in the warfarin group (Supplementary material online, *Figure S18A–D*), indicating that increased BMP2 signalling is due to the activation of p38. These results suggest that the high calcium condition leads to the lost affinity of SMOC1 binding to BMPR-II but not the binding to caveolin-1, which increases the formation of BMP-induced signalling complexes, endocytosis-associated BMP signalling, and p-p38 activation.

4. Discussion

The causes of AV calcification are complicated, and the most common types of clinical AV calcification include degeneration, diabetes, and chronic kidney disease. Increased serum calcium is frequent in chronic kidney disease patients receiving vitamin D3 treatment or complicated with secondary hyperparathyroidism.[27,28] In the present study, we explored the effects of SMOC1 on AVIC calcification under normal (~3 mmol/L) and high calcium (~5 mmol/L) conditions (Supplementary material online, *Table S1*). To our best knowledge, SMOC1 is the first protein that exerts dual effects on AVIC calcification in a high-calcium-dependent manner. SMOC1 has been previously reported to be a BMP/Smad1/5 signalling inhibitor in *Xenopus* and fibroblast cells[16] and acts as a negative regulator of ALK5/Smad2 signalling in the angiogenesis of endothelial cells.[29] Recently, Thomas et al reported that SMOC enhances BMP2 signalling via its EC domain binding to heparan sulphate proteoglycans (HSPGs).[30] In contrast to the role of the EC domain in enhancing BMP2 signalling in Thomas's study, we identified that the EC domain is essential for the inhibitory effect on the BMP2 signalling of SMOC1 in AVIC calcification. The loss of the BMPR-II binding function of SMOC1 by the EC domain under the high calcium condition enhanced BMP2/Smad1/5 signalling by increasing endocytosis and p38 activation. Our study indicates that SMOC1 plays various roles during the regulation of BMP2 signalling under different conditions, and how high calcium condition leads to the lost affinity of SMOC1 binding to BMPR-II needs further investigations.

BMP members are involved in vascular and valve calcification caused by different conditions. Matrix gla protein is a well-known studied endogenous BMP inhibitor in AV or vascular calcification.[31] *Xenopus* SMOC1 has been reported as a BMP antagonist involved in BMP receptor activation during development,[16] but the detailed mechanism underlying how SMOC1 inhibits BMP signalling in mammalian AVICs is unclear. Osteogenic differentiation induced by BMP2 is involved in AVIC calcification,[13] and there are four forms of type I receptors, ALK1, ALK2, ALK3 (also called BMPR-Ia), and ALK6 (also called BMPR-Ib), and three forms of type II receptors, BMPR-II, ActR-II and ActR-IIB which are involved in BMP signalling.[32] BMPR-II is unique among these receptors because of its long C-terminal domain (CTD), which is dispensable for canonical SMAD-mediated signalling.[33,34] Classically, BMPR-II activates type I BMP receptor kinases, which are critical for intracellular signal transduction.[35,36] Previous studies have reported that BMP receptor activation occurs following ligand binding to preformed receptor complexes (PFCs) or BMP-induced signalling complexes (BISCs) comprising BMPR-I and BMPR-II. The binding of BMP-2 to PFCs results in activation of Smad1/5 signalling, whereas BISCs initiate the activation of p38-dependent pathways through caveolin-mediated endocytosis.[26] Our data demonstrated that SMOC1 directly binds to BMPR-II only after ligand stimulation, resulting in the decreased activation of p38, and SMOC1 lost its affinity to BMPR-II but enhanced its signal transduction to the activation of p38 MAPK under the high calcium condition. Our data suggest that SMOC1 only regulates BISC-induced BMP2 signal transduction. Under the high calcium condition, SMOC1 preserves the ability to bind to caveolin-1, resulting in increased endocytosis. Similar to the reported proteins that could bind to the intracellular domain of BMPR-II and affect its function, such as SMYD2 binding to the kinase domain of BMPR-II or FMRP, a translational repressor,[37,38] our data demonstrated that endothelial cells secrete SMOC1, which enters the AVIC cytoplasm and then interacts with the intracellular domain of BMPR-II in AVICs. Our data showed that SMOC1 does not affect the binding ratio of BMP2 to BMP receptors under the pro-calcific condition. We speculated that SMOC1 binding to BMPR-II might affect the crosstalk between BISCs and p38 activation. The identification of the potential motif of the domain of BMPR-II to which SMOC1 binds warrants further study.

To reveal the structural basis of SMOC1 binding to BMPR-II, we identified that amino acids 372–383 of the EF-hand calcium-binding (EC) domain are required for the interaction of SMOC1 with BMPR-II and SMOC1-mediated inhibition of BMP2 signalling in AVICs. Our results differ from those in a previous study reporting the dispensable role of the *Xenopus* SMOC EC domain in BMP2 signalling.[30] Our results identified that the EC domain is essential for the binding of human SMOC1 to BMPR-II in AVICs under the pro-calcific condition because mutant SMOC1 with the mutation of amino acids 372–383 of the EC domain lost the ability to inhibit BMP2 signalling. We speculate that the different pathological statuses and associated structural changes of SMOC1 may contribute to the different roles of the SMOC1 EC domain in regulating BMP2 signalling. The EF-hand calcium-binding motif plays an important role in eukaryotic cell signal transduction. EF-hand proteins can be functionally divided into two classes: calcium sensors and calcium buffers. Calcium sensors translate the chemical signal of an increased calcium concentration into diverse biochemical and biological responses.[39] Calcium buffers are a smaller subset exemplified by calbindin D9K and parvalbumin, proteins that help to modulate the calcium signal both temporally and spatially because they bind free calcium to transmit the signal throughout the cell or to remove the potentially harmful ion from the cytoplasm.[40,41] SMOC1 is lesser-known EF-hand protein that also contains an EC motif. Whether SMOC1 acts as a calcium sensor or buffer protein remains unknown. Our data showed that SMOC1 promotes pAVIC apoptosis under the high calcium condition, suggesting that SMOC1 may be a calcium sensor and translate high-calcium-mediated pro-apoptotic and pro-osteogenic signalling into pAVICs. Further studies on the cell signal transduction mediated by SMOC1 may reveal the role of the EC domain. Although we demonstrated that SMOC1 loses its affinity to BMPR-II, how high extracellular calcium leads to the structural changes of the EC motif warrants further structural protein studies.

In conclusion, our work identifies the dual role of SMOC1 in AV calcification under normal and high calcium conditions. Our results indicate the complexity of BMP receptor-mediated signalling under different extracellular calcium contexts and suggest that much more attention should be given to the signal transduction mediated by BMP receptors under the different calcium concentrations. Our study suggests that serum calcium haemostasis disorder should be considered when the clinical therapeutic strategy is designed to target BMP receptors.

Highlights

- SMOC1 is mainly expressed by aortic valve endothelial cells, and the protein level of SMOC1 is decreased in human calcific aortic valve tissues.
- SMOC1 inhibits warfarin- or osteogenic medium-induced AVIC calcification but promotes high-calcium-medium-induced AVIC calcification *in vitro* and *in vivo*.
- SMOC1 inhibits p-p38-dependent BMP2 signal transduction by binding to BMPR-II with amino acids 372–383 of its EC domain.
- SMOC1 loses its ability to bind to BMPR-II but preserves its binding to caveolin-1 under high-extracellular-calcium conditions, leading to increased BMPR-II expression and endocytosis.

Supplementary material

Supplementary material is available at *Cardiovascular Research* online.

Authors' contributions

W.S. and X.K. conceived the project and designed the experiments. Y.W., W.S., and X.K. wrote the manuscript. Y.W., J.G., A.D., and S.Z. performed most experiments. M.D. performed some animal and immunostaining experiments. R.Z., Y.L., and Y.J. assisted Y.W. with some experiments. R.Z. and Y.S. provided human aortic valve samples.

Conflict of interest: none declared.

Funding

This work was supported by grants from the National Natural Science Foundation of China (No. 81270298, 81570247, 81627802, and 81900442), National Key R&D Program of China (2019YFA0210100), the Priority Academic Program Development of Jiangsu Higher Education Institutions (PAPD), a Shuang Chuang Tuan Dui Award of the Jiangsu Province of China, the Natural Science Foundation of Jiangsu Province for Youth (Grant No. BK20141024), the Natural Science Research in Universities of Jiangsu Province (No. 18KJB320005), and the Postgraduate Research & Practice Innovation Program of Jiangsu Province (KYCX19_1154). Wei Sun is an Assistant Fellow at the Collaborative Innovation Center for Cardiovascular Disease Translational Medicine, and Xiangqing Kong is a Fellow at the Collaborative Innovation Center for Cardiovascular Disease Translational Medicine.

Data availability

The data underlying this article will be shared on reasonable request to the corresponding author.

References

1. Stewart BF, Siscovick D, Lind BK, Gardin JM, Gottdiener JS, Smith VE, Kitzman DW, Otto CM. Clinical factors associated with calcific aortic valve disease. Cardiovascular Health Study. *J Am Coll Cardiol* 1997;**29**:630–634.
2. Roberts WC, Ko JM. Frequency by decades of unicuspid, bicuspid, and tricuspid aortic valves in adults having isolated aortic valve replacement for aortic stenosis, with or without associated aortic regurgitation. *Circulation* 2005;**111**:920–925.
3. Helske S, Kupari M, Lindstedt KA, Kovanen PT. Aortic valve stenosis: an active atheroinflammatory process. *Curr Opin Lipidol* 2007;**18**:483–491.
4. Soini Y, Salo T, Satta J. Angiogenesis is involved in the pathogenesis of nonrheumatic aortic valve stenosis. *Hum Pathol* 2003;**34**:756–763.
5. Hinton RB Jr, Lincoln J, Deutsch GH, Osinska H, Manning PB, Benson DW, Yutzey KE. Extracellular matrix remodeling and organization in developing and diseased aortic valves. *Circ Res* 2006;**98**:1431–1438.
6. Mohler ER, 3rd, Gannon F, Reynolds C, Zimmerman R, Keane MG, Kaplan FS. Bone formation and inflammation in cardiac valves. *Circulation* 2001;**103**:1522–1528.
7. Taylor PM, Batten P, Brand NJ, Thomas PS, Yacoub MH. The cardiac valve interstitial cell. *Int J Biochem Cell Biol* 2003;**35**:113–118.
8. Liu AC, Joag VR, Gotlieb AI. The emerging role of valve interstitial cell phenotypes in regulating heart valve pathobiology. *Am J Pathol* 2007;**171**:1407–1418.
9. Yamaguchi A, Katagiri T, Ikeda T, Wozney JM, Rosen V, Wang EA, Kahn AJ, Suda T, Yoshiki S. Recombinant human bone morphogenetic protein-2 stimulates osteoblastic maturation and inhibits myogenic differentiation *in vitro*. *J Cell Biol* 1991;**113**:681–687.
10. Katagiri T, Yamaguchi A, Komaki M, Abe E, Takahashi N, Ikeda T, Rosen V, Wozney JM, Fujisawa-Sehara A, Suda T. Bone morphogenetic protein-2 converts the differentiation pathway of C2C12 myoblasts into the osteoblast lineage. *J Cell Biol* 1994;**127**:1755–1766.
11. Osman L, Yacoub MH, Latif N, Amrani M, Chester AH. Role of human valve interstitial cells in valve calcification and their response to atorvastatin. *Circulation* 2006;**114**:547–552.
12. Kaden JJ, Bickelhaupt S, Grobholz R, Vahl CF, Hagl S, Brueckmann M, Haase KK, Dempfle CE, Borggrefe M. Expression of bone sialoprotein and bone morphogenetic protein-2 in calcific aortic stenosis. *J Heart Valve Dis* 2004;**13**:560–566.
13. Yang X, Meng X, Su X, Mauchley DC, Ao L, Cleveland JC Jr, Fullerton DA. Bone morphogenic protein 2 induces Runx2 and osteopontin expression in human aortic valve interstitial cells: role of Smad1 and extracellular signal-regulated kinase 1/2. *J Thorac Cardiovasc Surg* 2009;**138**:1008–1015.
14. Wirrig EE, Hinton RB, Yutzey KE. Differential expression of cartilage and bone-related proteins in pediatric and adult diseased aortic valves. *J Mol Cell Cardiol* 2011;**50**:561–569.
15. Vannahme C, Smyth N, Miosge N, Gosling S, Frie C, Paulsson M, Maurer P, Hartmann U. Characterization of SMOC-1, a novel modular calcium-binding protein in basement membranes. *J Biol Chem* 2002;**277**:37977–37986.
16. Thomas JT, Canelos P, Luyten FP, Moos M Jr, Xenopus SMOC-1 inhibits bone morphogenetic protein signaling downstream of receptor binding and is essential for postgastrulation development in Xenopus. *J Biol Chem* 2009;**284**:18994–19005.
17. Okada I, Hamanoue H, Terada K, Tohma T, Megarbane A, Chouery E, Abou-Ghoch J, Jalkh N, Cogulu O, Ozkinay F, Horie K, Takeda J, Furuichi T, Ikegawa S, Nishiyama K, Miyatake S, Nishimura A, Mizuguchi T, Niikawa N, Hirahara F, Kaname T, Yoshiura K-I, Tsurusaki Y, Doi H, Miyake N, Furukawa T, Matsumoto N, Saitsu H. SMOC1 is essential for ocular and limb development in humans and mice. *Am J Hum Genet* 2011;**88**:30–41.
18. Abouzeid H, Boisset G, Favez T, Youssef M, Marzouk I, Shakankiry N, Bayoumi N, Descombes P, Agosti C, Munier FL, Schorderet DF. Mutations in the SPARC-related modular calcium-binding protein 1 gene, SMOC1, cause Waardenburg anophthalmia syndrome. *Am J Hum Genet* 2011;**88**:92–98.
19. Rainger J, van Beusekom E, Ramsay JK, McKie L, Al-Gazali L, Pallotta R, Saponari A, Branney P, Fisher M, Morrison H, Bicknell L, Gautier P, Perry P, Sokhi K, Sexton D, Bardakjian TM, Schneider AS, Elcioglu N, Ozkinay F, Koenig R, Megarbane A, Semerci CN, Khan A, Zafar S, Hennekam R, Sousa SB, Ramos L, Garavelli L, Furga AS, Wischmeijer A, Jackson IJ, Gillessen-Kaesbach G, Brunner HG, Wieczorek D, van Bokhoven H, Fitzpatrick DR. Loss of the BMP antagonist, SMOC-1, causes Ophthalmo-acromelic (Waardenburg Anophthalmia) syndrome in humans and mice. *PLoS Genet* 2011;**7**:e1002114.
20. Choi YA, Lim J, Kim KM, Acharya B, Cho JY, Bae YC, Shin HI, Kim SY, Park EK. Secretome analysis of human BMSCs and identification of SMOC1 as an important ECM protein in osteoblast differentiation. *J Proteome Res* 2010;**9**:2946–2956.
21. Sun W, Zhao R, Yang Y, Wang H, Shao Y, Kong X. Comparative study of human aortic and mitral valve interstitial cell gene expression and cellular function. *Genomics* 2013;**101**:326–335.
22. Gao L, Ji Y, Lu Y, Qiu M, Shen Y, Wang Y, Kong X, Shao Y, Sheng Y, Sun W. Low-level overexpression of p53 promotes warfarin-induced calcification of porcine aortic valve interstitial cells by activating Slug gene transcription. *J Biol Chem* 2018;**293**:3780–3792.
23. Pluck A, Klasen C. Generation of chimeras by microinjection. *Methods Mol Biol* 2009;**561**:199–217.
24. Gu J, Lu Y, Deng M, Qiu M, Tian Y, Ji Y, Zong P, Shao Y, Zheng R, Zhou B, Sun W, Kong X. Inhibition of acetylation of histones 3 and 4 attenuates aortic valve calcification. *Exp Mol Med* 2019;**51**:1–14.
25. Kimura N, Matsuo R, Shibuya H, Nakashima K, Taga T. BMP2-induced apoptosis is mediated by activation of the TAK1-p38 kinase pathway that is negatively regulated by Smad6. *J Biol Chem* 2000;**275**:17647–17652.
26. Nohe A, Hassel S, Ehrlich M, Neubauer F, Sebald W, Henis YI, Knaus P. The mode of bone morphogenetic protein (BMP) receptor oligomerization determines different BMP-2 signaling pathways. *J Biol Chem* 2002;**277**:5330–5338.
27. Rodriguez M, Martinez-Moreno JM, Rodríguez-Ortiz ME, Muñoz-Castañeda JR, Almaden Y. Vitamin D and vascular calcification in chronic kidney disease. *Kidney Blood Press Res* 2011;**34**:261–268.

28. Tarrass F, Benjelloun M, Zamd M, Medkouri G, Hachim K, Benghanem MG, Ramdani B. Heart valve calcifications in patients with end-stage renal disease: analysis for risk factors. *Nephrology (Carlton)* 2006;**11**:494–496.
29. Awwad K, Hu J, Shi L, Mangels N, Abdel Malik R, Zippel N, Fisslthaler B, Eble JA, Pfeilschifter J, Popp R, Fleming I. Role of secreted modular calcium-binding protein 1 (SMOC1) in transforming growth factor beta signalling and angiogenesis. *Cardiovasc Res* 2015;**106**:284–294.
30. Thomas JT, Eric Dollins D, Andrykovich KR, Chu T, Stultz BG, Hursh DA, Moos M. SMOC can act as both an antagonist and an expander of BMP signaling. *Elife* 2017;**6**:e17935.
31. Herrmann SM, Whatling C, Brand E, Nicaud V, Gariepy J, Simon A, Evans A, Ruidavets JB, Arveiler D, Luc G, Tiret L, Henney A, Cambien F. Polymorphisms of the human matrix gla protein (MGP) gene, vascular calcification, and myocardial infarction. *Arterioscler Thromb Vasc Biol* 2000;**20**:2386–2393.
32. Katagiri T, Tsukamoto S. The unique activity of bone morphogenetic proteins in bone: a critical role of the Smad signaling pathway. *Biol Chem* 2013;**394**:703–714.
33. Foletta VC, Lim MA, Soosairajah J, Kelly AP, Stanley EG, Shannon M, He W, Das S, Massague J, Bernard O, Soosairaiah J. Direct signaling by the BMP type II receptor via the cytoskeletal regulator LIMK1. *J Cell Biol* 2003;**162**:1089–1098.
34. Lee-Hoeflich ST, Causing CG, Podkowa M, Zhao X, Wrana JL, Attisano L. Activation of LIMK1 by binding to the BMP receptor, BMPRII, regulates BMP-dependent dendritogenesis. *EMBO J* 2004;**23**:4792–4801.
35. Miyazono K, Kamiya Y, Morikawa M. Bone morphogenetic protein receptors and signal transduction. *J Biochem* 2010;**147**:35–51.
36. Aoki H, Fujii M, Imamura T, Yagi K, Takehara K, Kato M, Miyazono K. Synergistic effects of different bone morphogenetic protein type I receptors on alkaline phosphatase induction. *J Cell Sci* 2001;**114**:1483–1489.
37. Gao S, Wang Z, Wang W, Hu X, Chen P, Li J, Feng X, Wong J, Du JX. The lysine methyltransferase SMYD2 methylates the kinase domain of type II receptor BMPR2 and stimulates bone morphogenetic protein signaling. *J Biol Chem* 2017;**292**:12702–12712.
38. Broihier HT. BMP signaling turns up in fragile X syndrome: FMRP represses BMPR2. *Sci Signal* 2016;**9**:fs12.
39. Gifford JL, Walsh MP, Vogel HJ. Structures and metal-ion-binding properties of the Ca2+-binding helix-loop-helix EF-hand motifs. *Biochem J* 2007;**405**:199–221.
40. Akke M, Skelton NJ, Kordel J, Palmer AG, 3rd, Chazin WJ. Effects of ion binding on the backbone dynamics of calbindin D9k determined by 15N NMR relaxation. *Biochemistry* 1993;**32**:9832–9844.
41. Cox JA, Durussel I, Scott DJ, Berchtold MW. Remodeling of the AB site of rat parvalbumin and oncomodulin into a canonical EF-hand. *Eur J Biochem* 1999;**264**:790–799.

Translational perspective

Calcific aortic valve disease (CAVD) is the most common form of heart valve disease in developed countries. The limited understanding of the causes and pathogenesis of CAVD means that there is currently no effect medication available for clinic management. We report that SMOC1 regulated AVIC calcification by interfering with BMPR-II and p38 MAPK signalling. Our study demonstrates the complexity of BMP receptor-mediated signalling under different extracellular calcium contexts and suggests that serum calcium haemostasis disorder should be considered when the clinical therapeutic strategy is designed to target BMP receptors. Our study also suggests that p38 activation plays a key role during the formation of CAVD that may be a promising therapeutic target for CAVD.